A Bayesian Parametric Test for Multichannel Adaptive Signal Detection in Nonhomogeneous Environments

Pu Wang, *Student Member, IEEE*, Hongbin Li, *Senior Member, IEEE*, and Braham Himed, *Fellow, IEEE*

***Abstract*—This paper considers the problem of knowledge-aided space-time adaptive processing (STAP) in nonhomogeneous environments, where the covariance matrices of the training and test signals are assumed random and different from each other. A Bayesian detector is proposed by incorporating some *a priori* knowledge of the disturbance covariance matrices, and exploring their inherent block-Toeplitz structure. Specifically, the block-Toeplitz structure of the covariance matrix allows us to model the training signals as a multichannel auto-regressive (AR) process. The resulting detector is referred to as the Bayesian parametric adaptive matched filter (B-PAMF) which, compared with nonparametric Bayesian detectors, entails a lower training requirement and alleviates the computational complexity. Numerical results show that the proposed B-PAMF detector outperforms the standard PAMF test in nonhomogeneous environments.**

***Index Terms*—Bayesian detection, nonhomogeneous environments, parametric adaptive matched filter, space-time adaptive signal processing.**

I. Introduction

TRADITIONAL space-time adaptive processing (STAP) usually assumes a homogeneous environment, where the test signal shares the same covariance matrix with the training signals [1]. For nonhomogeneous environments, several models have been proposed. One involves partial homogeneity, by which the training signals share the covariance matrix with the test signal up to an unknown scaling factor [2]. This model is a special case of the generalized eigenrelation (GER) approach [3]. Another one is the compound Gaussian model, which models the training signals as a product of a texture (scalar) and a Gaussian vector. The texture is used to simulate power differences among the signals from different range bins [4]. More recently, a new class of Bayesian nonhomogeneous models for adaptive signal detection are introduced. The idea is to treat the covariance matrices of the test signal and training signals as random matrices that are related to one another through some probabilistic model but, in general, different in probability one [5]–[8].

Specifically, by employing a Bayesian nonhomogeneous model, a Bayesian adaptive matched filter (B-AMF) is proposed in [6]. The B-AMF detector replaces the standard sample covariance matrix with a maximum a posteriori (MAP) estimate [6]. It is shown that, by taking into account the heterogeneity, the B-AMF detector outperforms the standard AMF in the nonhomogeneous environment. For STAP application, the B-AMF detector still requires a significant amount of training signals. Consider, for example, the KASSPER [9], a widely used nonhomogeneous dataset. With $J=11$ spatial channels, $N=32$ coherent pulses and an instantaneous RF bandwidth of 500 KHz as in the KASSPER dataset, the B-AMF detector requires a minimum $K=JN=352$ training signals corresponding to a training range over 200 km, which might not be practical [9].

In this paper, while also adopting a Bayesian nonhomogeneous model, we further explore the inherent block-Toeplitz structure of the spatial–temporal covariance matrix which allows the disturbance (i.e., clutter and noise) to be modeled as a multichannel auto-regressive (AR) process [10], [11]. The resulting Bayesian parametric adaptive matched filter (B-PAMF) replaces the joint spatial-temporal whitening employed by the nonparametric B-AMF with successive spatial and temporal whitening. As such, it requires significantly less training and computation power, thus facilitating applications in nonhomogeneous environments.

II. Signal Model

Consider a radar system that employs J spatial channels, N temporal pulses, and K training range cells. The problem of interest is to detect a multichannel signal $\mathbf{s}(n) \in \mathbb{C}^{J\times 1}$, $n=0,1,\ldots,N-1$, with *unknown* amplitude α in the presence of spatially and temporally correlated disturbance $\mathbf{d}_0(n)$ [11]:

$$\begin{aligned} H_0 &: \mathbf{x}_0(n) = \mathbf{d}_0(n),\ n=0,1,\ldots,N-1, \\ H_1 &: \mathbf{x}_0(n) = \alpha\mathbf{s}(n) + \mathbf{d}_0(n),\ n=0,1,\ldots,N-1 \end{aligned} \quad (1)$$

where $\mathbf{x}_0(n)$ is the test signal. Besides $\mathbf{x}_0(n)$, there exist a set of target-free training signals $\mathbf{x}_k(n)=\mathbf{d}_k(n)$, $k=1,2,\ldots,K$, to assist the detection. In this paper, the signal model uses the following assumptions.

- **AS1 (Multichannel AR Process):** The disturbances in both the test and training signals are modeled as a multichannel AR process [10], [11]:

$$\mathbf{d}_k(n) = -\sum_{i=1}^{P}\mathbf{A}^H(i)\mathbf{d}_k(n-i) + \boldsymbol{\varepsilon}_k(n),\ k=0,\ldots,K, \quad (2)$$

  where $\mathbf{A}^H = \left[\mathbf{A}^H(1), \mathbf{A}^H(2), \ldots, \mathbf{A}^H(P)\right]$ denotes the *unknown* multichannel AR coefficient matrix, and $\boldsymbol{\varepsilon}_k(n)$

Manuscript received September 24, 2009; revised December 02, 2009. First published December 31, 2009; current version published February 17, 2010. This work was supported by the Air Force Research Laboratory (AFRL) under Contract FA8750-05-2-0001 and the Air Force Office of Scientific Research (AFOSR) under Grant FA9550-09-1-0310. The associate editor coordinating the review of this manuscript and approving it for publication was Dr. Henry Leung.

P. Wang and H. Li are with the Department of Electrical and Computer Engineering, Stevens Institute of Technology, Hoboken, NJ 07030 USA (e-mail: pwang4@stevens.edu; hli@stevens.edu).

B. Himed is with AFRL/RYRT, Dayton, OH 45433 (e-mail: Braham.Himed@wpafb.af.mil).

Color versions of one or more of the figures in this paper are available online at http://ieeexplore.ieee.org.

Digital Object Identifier 10.1109/LSP.2009.2039380

denote the $J \times 1$ temporally white but spatially colored noise vectors.

- **AS2 (Random Spatial Covariance Matrix of Training Signals):**The noise vector $\boldsymbol{\varepsilon}_k(n)$, conditioned on $\mathbf{Q}$, is a zero-mean complex Gaussian variable, i.e., $\boldsymbol{\varepsilon}_k(n) \sim \mathcal{CN}(\mathbf{0}, \mathbf{Q})$. The random spatial covariance matrix $\mathbf{Q}$ follows an inverse complex Wishart distribution with degrees of freedom μ and mean $\bar{\mathbf{Q}}$ (c.f [6]):

$$p(\mathbf{Q}) = \frac{\left|(\mu - J)\bar{\mathbf{Q}}\right|^{\mu}}{\tilde{\Gamma}(J,\mu)\left|\mathbf{Q}\right|^{(\mu+J)}} e^{-(\mu-J)\mathrm{tr}\left(\mathbf{Q}^{-1}\bar{\mathbf{Q}}\right)} \quad (3)$$

where

$$\tilde{\Gamma}(J,\mu) = \pi^{J(J-1)/2} \prod_{k=1}^{J} \Gamma\left(\mu - J + k\right) \quad (4)$$

with Γ denoting the Gamma function [12].

- **AS3 (Random Spatial Covariance Matrix of Test Signal):**The noise vector in the test signal $\boldsymbol{\varepsilon}_0(n) \sim \mathcal{CN}(\mathbf{0}, \mathbf{Q}_0)$, and $\mathbf{Q}_0$, conditioned on $\mathbf{Q}$, has a complex Wishart distribution with degrees of freedom ν and mean $\mathbf{Q}$ (c.f [6]):

$$p\left(\mathbf{Q}_0|\mathbf{Q}\right) = \frac{\nu^{J\nu}|\mathbf{Q}_0|^{\nu-J}}{\tilde{\Gamma}(J,\nu)|\mathbf{Q}|^{\nu}} e^{-\nu\mathrm{tr}\left(\mathbf{Q}^{-1}\mathbf{Q}_0\right)}. \quad (5)$$

The multichannel AR process for the disturbances in both the test and training signals consists of two types of unknown parameters: one is the *deterministic* AR coefficient matrix $\mathbf{A}$, and the other is the *random* spatial covariance matrices $\mathbf{Q}$ and $\mathbf{Q}_0$. We exploit for detection a *prior* spatial covariance matrix $\bar{\mathbf{Q}}$, which is taken as the mean of $\mathbf{Q}$. This prior spatial covariance matrix $\bar{\mathbf{Q}}$ can be obtained by a block LDU decomposition [10] of a prior joint spatial-temporal covariance matrix $\bar{\mathbf{R}}$ derived from sources such as land-use maps, past measurements, etc. [9]. The importance of the *a priori* knowledge $\bar{\mathbf{Q}}$ is controlled by parameter μ, while the heterogeneity, i.e., the statistical difference between the test and training signals, is determined by parameter ν. Most importantly, $\mathbf{Q} \neq \mathbf{Q}_0$ with probability one, which ensures that the environment is nonhomogeneous [6].

III. Bayesian Parametric Adaptive Matched Filter

If parameters $\mathbf{A}$ and $\mathbf{Q}_0$ are known, the solution to the problem of interest is the classical parametric matched filter (PMF) [10]:

$$T_{\mathrm{PMF}} = \frac{\left|\sum_{n=P}^{N-1} \tilde{\mathbf{s}}^H(n)\mathbf{Q}_0^{-1}\tilde{\mathbf{x}}_0(n)\right|^2}{\sum_{n=P}^{N-1} \tilde{\mathbf{s}}^H(n)\mathbf{Q}_0^{-1}\tilde{\mathbf{s}}(n)} \underset{H_0}{\overset{H_1}{\gtrless}} \gamma_{\mathrm{PMF}} \quad (6)$$

where γ_{PMF} denotes the PMF threshold subject to a selected probability of false alarm. The whitened steering vector and test signal are obtained by using the true AR coefficient matrix $\mathbf{A}$

$$\tilde{\mathbf{s}}(n) = \mathbf{s}(n) + \sum_{p=1}^{P} \mathbf{A}^H(p)\mathbf{s}(n-p), \quad (7)$$

$$\tilde{\mathbf{x}}_0(n) = \mathbf{x}_0(n) + \sum_{p=1}^{P} \mathbf{A}^H(p)\mathbf{x}_0(n-p). \quad (8)$$

For practical scenarios with unknown $\mathbf{A}$ and $\mathbf{Q}_0$, the parametric AMF (PAMF) replaces the exact $\mathbf{A}$ and $\mathbf{Q}_0$ in the PMF statistic by their estimates, e.g., the maximum likelihood estimate (MLE) obtained from training signals. For the nonhomogeneous environment considered here, we take into account the uncertainty of the spatial covariance matrix and adapt a hybrid PAMF approach. The resulting detector is referred to as the Bayesian PAMF (B-PAMF). It is obtained by first finding the MLE of the deterministic AR coefficient matrix $\hat{\mathbf{A}}_{\mathrm{ML}}$ from the training data and then the maximum *a posteriori* (MAP) estimate of the stochastic spatial covariance matrix $\hat{\mathbf{Q}}_{0,\mathrm{MAP}}$ conditioned on the ML estimate $\hat{\mathbf{A}}_{\mathrm{ML}}$. Finally, we use them to replace $\mathbf{A}$ and $\mathbf{Q}_0$ in the PMF statistic.

A. MLE of $\mathbf{A}$

Denote $\mathbf{x}_k \triangleq [\mathbf{x}_k^T(0), \mathbf{x}_k^T(1), \ldots, \mathbf{x}_k^T(N-1)]^T \in \mathbb{C}^{JN\times 1}$. According to the signal model, the joint conditional probability density function (pdf) of the training signals can be written as [11]

$$f\left(\mathbf{x}_1, \ldots, \mathbf{x}_K|\mathbf{A}, \mathbf{Q}\right) = \left[\frac{1}{\pi^J\left|\mathbf{Q}\right|} e^{-\mathrm{tr}\left(\mathbf{Q}^{-1}\boldsymbol{\Sigma}(\mathbf{A})\right)}\right]^{K(N-P)},$$

where

$$\boldsymbol{\Sigma}(\mathbf{A}) = \frac{1}{K(N-P)} \sum_{k=1}^{K}\sum_{n=P}^{N-1} \boldsymbol{\varepsilon}_k(n)\boldsymbol{\varepsilon}_k^H(n). \quad (9)$$

From **AS2** , we can remove the dependence of the above pdf on $\mathbf{Q}$ by integrating it over $\mathbf{Q}$:

$$\begin{aligned} f\left(\mathbf{x}_1, \ldots, \mathbf{x}_K|\mathbf{A}\right) &= \int f\left(\mathbf{x}_1, \ldots, \mathbf{x}_K|\mathbf{A}, \mathbf{Q}\right) p(\mathbf{Q}) d\mathbf{Q} \\ &= \frac{\left|(\mu-J)\bar{\mathbf{Q}}\right|^{\mu}}{\pi^{JK(N-P)}\tilde{\Gamma}(J,\mu)} \int |\mathbf{Q}|^{-L} e^{-\mathrm{tr}\left(\mathbf{Q}^{-1}\tilde{\boldsymbol{\Sigma}}\right)} d\mathbf{Q} \\ &= \frac{\left|(\mu-J)\bar{\mathbf{Q}}\right|^{\mu}\tilde{\Gamma}(J, L-J)}{\pi^{JK(N-P)}\tilde{\Gamma}(J,\mu)} |\tilde{\boldsymbol{\Sigma}}|^{-L+J} \end{aligned} \quad (10)$$

where

$$L = \mu + J + K(N-P), \quad (11)$$

and

$$\tilde{\boldsymbol{\Sigma}} = K(N-P)\boldsymbol{\Sigma}(\mathbf{A}) + (\mu - J)\bar{\mathbf{Q}}. \quad (12)$$

Therefore, finding the MLE of $\mathbf{A}$ is equivalent to minimizing the determinant of $\tilde{\boldsymbol{\Sigma}}$. Rewrite the matrix $\tilde{\boldsymbol{\Sigma}}$ as

$$\begin{aligned} \tilde{\boldsymbol{\Sigma}} &= K(N-P)\boldsymbol{\Sigma}(\mathbf{A}) + (\mu - J)\bar{\mathbf{Q}} \\ &= \hat{\mathbf{R}}_{xx} + \hat{\mathbf{R}}_{yx}^H\mathbf{A} + \mathbf{A}^H\hat{\mathbf{R}}_{yx} + \mathbf{A}^H\hat{\mathbf{R}}_{yy}\mathbf{A} \\ &\quad + (\mu - J)\bar{\mathbf{Q}} \\ &= \left(\mathbf{A}^H + \hat{\mathbf{R}}_{yx}^H\hat{\mathbf{R}}_{yy}^{-1}\right)\hat{\mathbf{R}}_{yy}\left(\mathbf{A}^H + \hat{\mathbf{R}}_{yx}^H\hat{\mathbf{R}}_{yy}^{-1}\right)^H \\ &\quad + \hat{\mathbf{R}}_{xx} - \hat{\mathbf{R}}_{yx}^H\hat{\mathbf{R}}_{yy}^{-1}\hat{\mathbf{R}}_{yx} + (\mu - J)\bar{\mathbf{Q}} \end{aligned} \quad (13)$$

where

$$\hat{\mathbf{R}}_{xx} = \sum_{k=1}^{K}\sum_{n=P}^{N-1} \mathbf{x}_k(n)\mathbf{x}_k^H(n), \quad (14)$$

$$\hat{\mathbf{R}}_{yy} = \sum_{k=1}^{K}\sum_{n=P}^{N-1} \mathbf{y}_k(n)\mathbf{y}_k^H(n), \quad (15)$$

$$\hat{\mathbf{R}}_{yx} = \sum_{k=1}^{K}\sum_{n=P}^{N-1} \mathbf{y}_k(n)\mathbf{x}_k^H(n) \tag{16}$$

with $\mathbf{y}_k(n) = \left[\mathbf{x}_k^T(n-1), \ldots, \mathbf{x}_k^T(n-P)\right]^T \in \mathbb{C}^{JP\times 1}$. Since $\hat{\mathbf{R}}_{yy}$ is nonnegative definite and the remaining terms $\hat{\mathbf{R}}_{xx} - \hat{\mathbf{R}}_{yx}^H\hat{\mathbf{R}}_{yy}^{-1}\hat{\mathbf{R}}_{yx} + (\mu - J)\bar{\mathbf{Q}}$ do not depend on $\mathbf{A}$, it follows from (13) that

$$\tilde{\boldsymbol{\Sigma}} \geq \tilde{\boldsymbol{\Sigma}}|_{\mathbf{A}=\hat{\mathbf{A}}_{\mathrm{ML}}} = \hat{\mathbf{R}}_{xx} - \hat{\mathbf{R}}_{yx}^H\hat{\mathbf{R}}_{yy}^{-1}\hat{\mathbf{R}}_{yx} + (\mu - J)\bar{\mathbf{Q}} \tag{17}$$

where the MLE of $\mathbf{A}$ is

$$\hat{\mathbf{A}}_{\mathrm{ML}}^H = -\hat{\mathbf{R}}_{yx}^H\hat{\mathbf{R}}_{yy}^{-1}. \tag{18}$$

When $\tilde{\boldsymbol{\Sigma}}$ is minimized, the MLE $\hat{\mathbf{A}}_{\mathrm{ML}}$ also minimizes any nondecreasing function including the determinant of $\tilde{\boldsymbol{\Sigma}}$. It is noted that the MLE $\hat{\mathbf{A}}_{\mathrm{ML}}$ involves training signals only. With the MLE of $\mathbf{A}$, the MAP estimate of $\mathbf{Q}_0$ is obtained in the following section.

B. MAP Estimate of $\mathbf{Q}_0$

The MAP estimate of $\mathbf{Q}_0$ requires the computation of the posterior distribution $f(\mathbf{Q}_0|\mathbf{x}_1, \mathbf{x}_2, \ldots, \mathbf{x}_K)$:

$$f(\mathbf{Q}_0|\mathbf{x}_1, \mathbf{x}_2, \ldots, \mathbf{x}_K) = \int f(\mathbf{Q}_0, \mathbf{Q}|\mathbf{x}_1, \mathbf{x}_2, \ldots, \mathbf{x}_K)d\mathbf{Q} \tag{19}$$

where

$$\begin{aligned} & f(\mathbf{Q}_0, \mathbf{Q}|\mathbf{x}_1, \mathbf{x}_2, \ldots, \mathbf{x}_K) \\ & \quad \propto f(\mathbf{x}_1, \mathbf{x}_2, \ldots, \mathbf{x}_K|\mathbf{Q}_0, \mathbf{Q})\, p(\mathbf{Q}_0|\mathbf{Q})\, p(\mathbf{Q}) \\ & \quad \propto |\mathbf{Q}_0|^{\nu-J}\, |\mathbf{Q}|^{-(L+\nu)}\, e^{-\mathrm{tr}\left(\mathbf{Q}^{-1}\left[\tilde{\boldsymbol{\Sigma}}+\nu\mathbf{Q}_0\right]\right)}. \end{aligned} \tag{20}$$

As a result, (19) can be calculated as

$$\begin{aligned} & \int f(\mathbf{Q}_0, \mathbf{Q}|\mathbf{x}_1, \mathbf{x}_2, \ldots, \mathbf{x}_K)d\mathbf{Q} \\ & \quad \propto |\mathbf{Q}_0|^{\nu-J} \int |\mathbf{Q}|^{-(L+\nu)}\, e^{-\mathrm{tr}\left(\mathbf{Q}^{-1}\left[\tilde{\boldsymbol{\Sigma}}+\nu\mathbf{Q}_0\right]\right)} d\mathbf{Q} \\ & \quad \propto |\mathbf{Q}_0|^{\nu-J}\, |\tilde{\boldsymbol{\Sigma}} + \nu\mathbf{Q}_0|^{\mu+\nu+K(N-P)}. \end{aligned} \tag{21}$$

Taking the derivative of the logarithm of the above equation with respect to $\mathbf{Q}_0$ and setting it to zero, we have (22), shown at the bottom of the page, which suggests that, for a given $\mathbf{A}$, the estimate of $\mathbf{Q}_0$ is

$$\hat{\mathbf{Q}}_0 = \frac{(\nu - J)}{\nu(\mu + J + K(N-P))}\tilde{\boldsymbol{\Sigma}}. \tag{23}$$

Replacing $\mathbf{A}$ with $\hat{\mathbf{A}}_{\mathrm{ML}}$ of (18) in the above estimate (viz, $\tilde{\boldsymbol{\Sigma}}$), the MAP estimate of $\mathbf{Q}_0$ is

$$\begin{aligned} \hat{\mathbf{Q}}_{0,\mathrm{MAP}} = & \frac{(\nu - J)}{\nu(\mu + J + K(N-P))} \\ & \times \left[\hat{\mathbf{R}}_{xx} - \hat{\mathbf{R}}_{yx}^H\hat{\mathbf{R}}_{yy}^{-1}\hat{\mathbf{R}}_{yx} + (\mu - J)\bar{\mathbf{Q}}\right]. \end{aligned} \tag{24}$$

Therefore, the MAP estimate of $\mathbf{Q}$ is a linear combination of a standard estimate of $\mathbf{Q}$ of [11] and the *a priori* knowledge $\bar{\mathbf{Q}}$. It is interesting to note that this linear combination is similar to those obtained for nonparametric approaches [6], [13].

C. Bayesian PAMF

With the ML estimate of $\mathbf{A}$ and the MAP estimate of $\mathbf{Q}_0$, the B-PAMF test is given by (c.f (6))

$$T_{\mathrm{B-PAMF}} = \frac{\left|\sum_{n=P}^{N-1} \hat{\tilde{\mathbf{s}}}^H(n)\hat{\mathbf{Q}}_{0,\mathrm{MAP}}^{-1}\hat{\tilde{\mathbf{x}}}_0(n)\right|^2}{\sum_{n=P}^{N-1} \hat{\tilde{\mathbf{s}}}^H(n)\hat{\mathbf{Q}}_{0,\mathrm{MAP}}^{-1}\hat{\tilde{\mathbf{s}}}(n)} \underset{H_0}{\overset{H_1}{\gtrless}} \gamma_{\mathrm{B-PAMF}} \tag{25}$$

where $\gamma_{\mathrm{B-PAMF}}$ denotes the B-PAMF test threshold, $\hat{\mathbf{Q}}_{0,\mathrm{MAP}}$ is given by (24), and the whitened steering vector and the whitened test signal are obtained by using (7) and (8) with $\mathbf{A}$ replaced by $\hat{\mathbf{A}}_{\mathrm{ML}}$ in (18).

From (25), it is seen that the B-PAMF performs successive whitening, i.e., temporal whitening followed by spatial whitening, as opposed to joint spatio-temporal whitening across all JN dimensions of the B-AMF [6]. On the other hand, compared with the standard PAMF [10], the B-PAMF detector incorporates the *a priori* knowledge, i.e., $\bar{\mathbf{Q}}$; in addition, the heterogeneity parameter ν and the importance parameter μ are employed to control how the *a priori* knowledge affects an updated MAP estimate of the spatial covariance matrix $\mathbf{Q}$. Hence, the B-PAMF detector achieves better computational efficiency and reduces the training requirement over the B-AMF. Meanwhile, by exploiting the *a priori* knowledge and a nonhomogeneous model, it yields improved detection performance over the PAMF detector, as shown next.

IV. Numerical Examples

In this section, simulation results are provided to illustrate the performance of the B-PAMF detector. The disturbance signal $\mathbf{d}_k$ is generated as a multichannel AR (2) process with AR coefficient $\mathbf{A}$ and a spatial covariance matrix $\mathbf{Q}$. The signal vector $\mathbf{s}$ corresponds to a uniform linear array with randomly selected normalized spatial and Doppler frequencies. The signal-to-interference-plus-noise ratio (SINR) is defined as

$$\mathrm{SINR} = |\alpha|^2\mathbf{s}^H\bar{\mathbf{R}}^{-1}\mathbf{s}, \tag{26}$$

where $\bar{\mathbf{R}}$ is the spatial-temporal covariance matrix of the AR process with AR coefficient matrix $\mathbf{A}$ and spatial covariance matrix $\bar{\mathbf{Q}}$. For each Monte-Carlo trial, the spatial covariance matrix $\mathbf{Q}$ for the training signal is generated from an inverse Wishart distribution with mean $\bar{\mathbf{Q}}$, and then, for each given $\mathbf{Q}$, the spatial covariance matrix $\mathbf{Q}_0$ for the test signal is generated from a Wishart distribution with mean $\mathbf{Q}$. Note that a similar process is used in [6] to generate the random covariance matrices.

$$\frac{\partial \ln f(\mathbf{Q}_0|\mathbf{x}_1, \mathbf{x}_2, \ldots, \mathbf{x}_K)}{\partial \mathbf{Q}_0} \propto (\nu - J)\mathbf{Q}_0^{-1} - \nu(\mu + \nu + K(N-P))\,[\tilde{\boldsymbol{\Sigma}} + \nu\mathbf{Q}_0]^{-1} = 0 \tag{22}$$

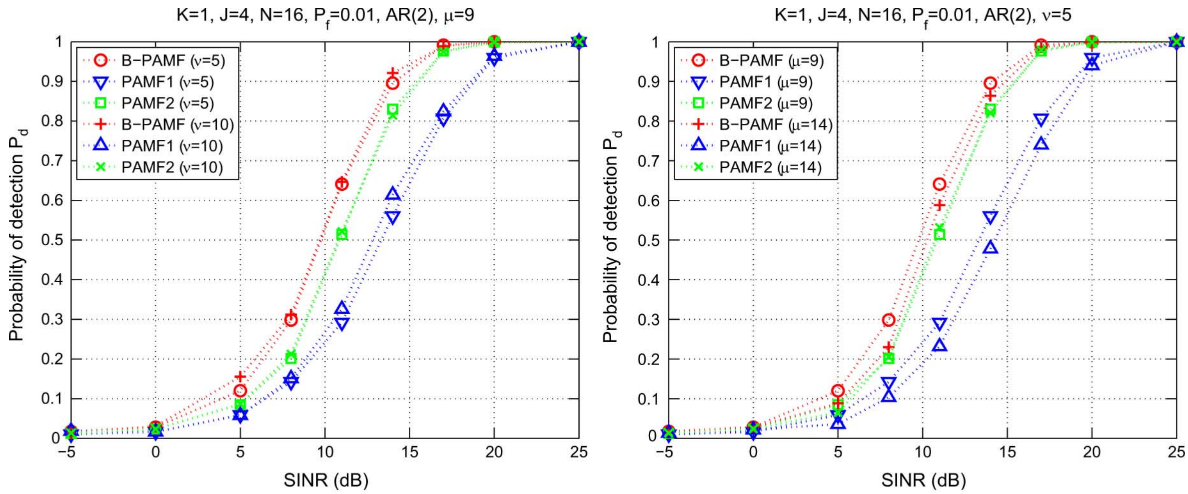

(a) (b)

Fig. 1. Probability of detection versus SINR when $J = 4$, $N = 16$, $P = 2$, $K = 1$, and $P_f = 0.01$ for cases of (a) $\mu = 9$; (b) $\nu = 5$.

In the above nonhomogeneous environment, we compare the B-PAMF with two PAMF detectors: 1) PAMF1: the original PAMF [10]; 2) PAMF2: the modified PAMF by using the data-independent prior knowledge $\bar{\mathbf{Q}}$ as an estimate of $\mathbf{Q}_0$. Fig. 1 shows the probability of detection versus the SINR for the three detectors in cases of different values of μ and ν, when $P = 2$, $J = 4$, $N = 16$, $K = 1$, and $P_f = 0.01$. It is seen that, in all cases, the B-PAMF outperforms the two PAMF detectors. In Fig. 1(a) of a fixed value of μ, we consider two values of $\nu : \nu = 5$ and $\nu = 10$. A larger value of ν means a smaller difference between the test and training signals and hence a more homogeneous environment. The simulations results show that, when $\nu = 10$, the B-PAMF and PAMF detectors perform slightly better than the case of $\nu = 5$. Specifically, for a probability of detection equal to 0.8, there is about 4 dB loss from the B-PAMF to the PAMF1 and 1 dB loss from the B-PAMF to the PAMF2. On the other hand, the effect of μ is examined in Fig. 1(b). As seen from **AS2** , increasing μ means that the spatial covariance matrix $\mathbf{Q}$ of the training signals are closer to the prior $\bar{\mathbf{Q}}$ and hence the more important the prior knowledge $\bar{\mathbf{Q}}$. In this case, the B-PAMF adapts to the environment change by putting more weight on the $\bar{\mathbf{Q}}$ in the MAP estimate of (24), while the original PAMF1 employs the same estimate of $\mathbf{Q}_0$. It turns out the performance gap between the B-PAMF and PAMF1 is enlarged from about 3.8 dB when $\mu = 9$ to about 4.5 dB when $\mu = 14$, as seen from Fig. 1(b). On the other hand, the PAMF2 benefits from using $\bar{\mathbf{Q}}$, which is a reliable prior estimate of $\mathbf{Q}_0$ and hence its performance is slightly improved as μ increases from 9 to 14.

V. Conclusion

A Bayesian parametric adaptive matched filter has been proposed by modeling the disturbances in the test and training signals as a multichannel AR process and characterizing the heterogeneity between the training and test signals via a random matrix model. The B-PAMF admits successive temporal and spatial whitening, which reduces the computational complexity of the joint spatial-temporal whitening based adaptive detectors. The training requirement is also reduced. Simulation results show that the B-PAMF detector is effective in nonhomogeneous environment.

References

[1] J. Ward, Space-Time Adaptive Processing for Airborne Radar Lincoln Laboratory, Mass. Inst. Technol., Cambridge, 1994, Tech. Rep. 1015.

[2] A. De Maio and S. Iommelli, "Coincidence of the rao test, wald test, and GLRT in partially homogenous environment," *IEEE Signal Process. Lett.*, vol. 15, pp. 385–388, 2008.

[3] C. D. Richmond, "Statistics of adaptive nulling and use of the generalized eigenrelation (GER) for modeling inhomogeneities in adaptive processing," *IEEE Trans. Signal Process.*, pp. 1263–1273, May 2000.

[4] J. H. Michels, B. Himed, and M. Rangaswamy, "Performance of STAP tests in Gaussian and compound-Gaussian clutter," *Digital Signal Process.*, vol. 10, no. 4, pp. 309–324, Oct. 2000.

[5] A. De Maio and A. Farina, "Adaptive radar detection: A Bayesian approach," in *Proc. 2006 Int. Radar Symp.*, Krakow, Poland, May 2006, pp. 85–88.

[6] O. Besson, J.-Y. Tourneret, and S. Bidon, "Knowledge-aided Bayesian detection in heterogeneous environment," *IEEE Signal Process. Lett.*, pp. 355–358, May 2007.

[7] A. De Maio, A. Farina, and G. Foglia, "Adaptive radar detection: A Bayesian approach," in *Proceedings of the 2007 IEEE Int. Conf. Radar*, Waltham, MA, Apr. 2007, pp. 624–629.

[8] S. Bidon, O. Besson, and J.-Y. Tourneret, "A Bayesian approach to adaptive detection in non-homogeneous environments," *IEEE Trans. Signal Process.*, pp. 205–217, Jan. 2008.

[9] J. S. Bergin and P. M. Techau, High-Fidelity Site-Specific Radar Simulation: KASSPER'02 Workshop Datacube Information Systems Laboratories, Inc., Vienna, VA, 2002, Tech. Rep. ISL-SCRD-TR-02-105.

[10] J. R. Román, M. Rangaswamy, D. W. Davis, Q. Zhang, B. Himed, and J. H. Michels, "Parametric adaptive matched filter for airborne radar applications," *IEEE Trans. Aerosp. Electron. Syst.*, vol. 36, pp. 677–692, Apr. 2000.

[11] K. J. Sohn, H. Li, and B. Himed, "Parametric GLRT for multichannel adaptive signal detection," *IEEE Trans. Signal Process.*, vol. 55, pp. 5351–5360, Nov. 2007.

[12] M. Abramowitz and I. A. Ryzhik, *Handbook of Mathematical Functions With Formulas Graphs, and Mathematical Tables*. New York: Dover, 1972.

[13] P. Stoica, J. Li, X. Zhu, and J. R. Guerci, "On using a priori knowledge in space-time adaptive processing," *IEEE Trans. Signal Process.*, pp. 2598–2602, Jun. 2008.